3D full-waveform inversion of the Snowflake CO_2 injection VSP data

Hyeong-Geun Ji[1], Sea-Eun Park[1], Ju-Won Oh[1] and Kris Innanen

1 Jeonbuk National University

ABSTRACT

The CaMI FRS is a pilot-scale demonstration carbon capture and storage (CCS) project aimed at validating 4D seismic monitoring. This report focuses on verifying the suitability of 3D acoustic full-waveform inversion (FWI) for inverting Snowflake vertical seismic profile (VSP) data acquired from CaMI FRS both before and after CO_2 injection. The Snowflake data is obtained by a walk-away and walk-around VSP survey, which is applicable to both 2D and 3D FWI. Initially, we present the results of 2D acoustic FWI along each walk-away shot line. Then, we show the results of 3D acoustic FWI utilizing the complete 3D VSP dataset. While the inverted models from 2D FWI did not meet expectations, the inverted model from 3D FWI yields a more satisfactory geological representation in terms of layer continuity and noise reduction. Moreover, the changes in P-wave velocity are partially detected from the individual 3D FWI results for the Snowflake data before and after CO_2 injection.

INTRODUCTION

Carbon capture and storage (CCS) is a crucial technology for mitigating global warming by directly reducing a significant amount of CO_2 emission. In the CCS project, to minimize the risk of CO_2 leakage stored in a reservoir, it is indispensable to monitor the behavior of injected CO_2. Among various geophysical methods for monitoring CO_2, the time-lapse seismic survey, which interprets changes in reflected seismic waves resulting from injected CO_2, is widely utilized due to its high resolution, enabling the acquisition of detailed underground structural images. However, seismic waves are highly sensitive to ambient noise caused by human activities and the surrounding environment. In the case of onshore land data, surface waves and microseisms from the Earth analyze seismic wave data more complicated. In addition, non-repeatability from acquisition geometry in two different seismic surveys before and after injection causes 4D noise. To address these challenges and improve the state of CO_2 monitoring technology, the Containment and Monitoring Institute (CaMI) project was launched under Carbon Management Canada (CMC), and various monitoring research projects are ongoing in the Field Research Station (FRS).

CaMI is a pilot-scale project for the validation of CO_2 monitoring technology. The vertical seismic profile (VSP) method, which deploys receivers in a borehole to acquire seismic data, was primarily employed to monitor injected CO_2 in this facility. This method mainly focuses on monitoring changes in underground properties rather than implementing subsurface structures. Its applicability has been validated in the Otway project launched in Australia by CO2CRC (Egorov et al., 2018). Because the receivers are deployed on the borehole, they can directly acquire the seismic signals reflected from the plume. It can also reduce the influence of surface waves, regarded as noise. Furthermore, non-repeatability can be minimized because the fixed receivers record seismic rays following similar paths.

Full waveform inversion (FWI) is one of the crucial methods used to estimate underground properties by minimizing the residual between observed data and predicted data through iterative processes (Tarantola, 1984). Although this technique requires a lot of calculations, it is effective because it allows the estimation of underground characteristics with high resolution. Previously, studies on CaMI FRS mainly focused on synthetic 2D FWI for monitoring feasibility verification (Amundaray et al., 2020), real data application for applicability verification of 2D elastic FWI (Eaid et al., 2021), technology development in FWI for accuracy improvement (Cai et al., 2022), and estimation of rock physics properties (Hu and Innanen, 2022). However, to monitor CO_2 plumes along azimuth direction with high accuracy, 3D FWI should be considered.

In this study, we apply 2D and 3D acoustic FWI in the time domain with VSP data acquired from CaMI FRS in 2018 and 2022, referred to as Snowflake I and II, respectively. The 3D FWI requires significant computational resources, so we only consider acoustic FWI in this work. Firstly, we compare the results of 3D FWI with those of 2D acoustic FWI along each shot line. Then, we verify the applicability of 4D time-lapse monitoring based on FWI by individually applying 3D acoustic FWI for before and after injection data

SNOWFLAKE DATA

The CaMI FRS (Containment and Monitoring Institutes Field Research Station) is located near Brooks, southern Alberta. The purpose of the CaMI FRS is developing and validating the monitoring technologies to monitor injected CO_2 (Eaid et al., 2021). Figure 1 shows the acquisition geometry of VSP data acquired in CaMI FRS, referred to as Snowflake data. The observation well for geophysical monitoring is located 20 m southwest of the injection well, and the 3C geophones are cemented outside of the casing with 1 - 2 m intervals from the surface to 324 m in depth. The target for CO_2 injection at CaMI FRS is the Basal Belly River Sandstone (BBRS) formation, which was formed during the late Cretaceous period. This formation is an extremely thin layer with a thickness of 7 m, located at a depth of 295 m to 302 m and the caprock that seals the injected CO_2 is composed of coals and mixed shale and sandstone units (Macquet et al., 2019).

In 2018, before injection (Snowflake I data), a walk-away and walk-around VSP survey was conducted to acquire baseline data with a total of 12 shot lines at 15-degree intervals centered around the geophysics well (Hall et al., 2018). In Figure 1, along four main shot lines (Lines 1, 4, 7, 10), the shots were vibrated at approximately 10 m intervals, while, along other lines, the shots were vibrated at approximately 60 m intervals. In 2022, after CO_2 injection (Snowflake II data), the monitoring survey was conducted following almost the same geometry as the baseline survey.

Because the changes in rigidity and density resulting from CO_2 injection are relatively small, thus, the goal of our time-lapse FWI is detecting the reduction in P-wave velocity after CO_2 injection. In addition, because the BBRS is a 10 m thick aquifer, we require higher frequency components in 3D FWI. For these reasons, to efficiently monitor CO_2 behavior by reducing the computational resources required in 3D FWI, we focus on acoustic FWI for time-lapse monitoring. To build initial 3D background model (Figure 2), we used smoothed 1D velocity model from well-log information (Hu et al., 2022).

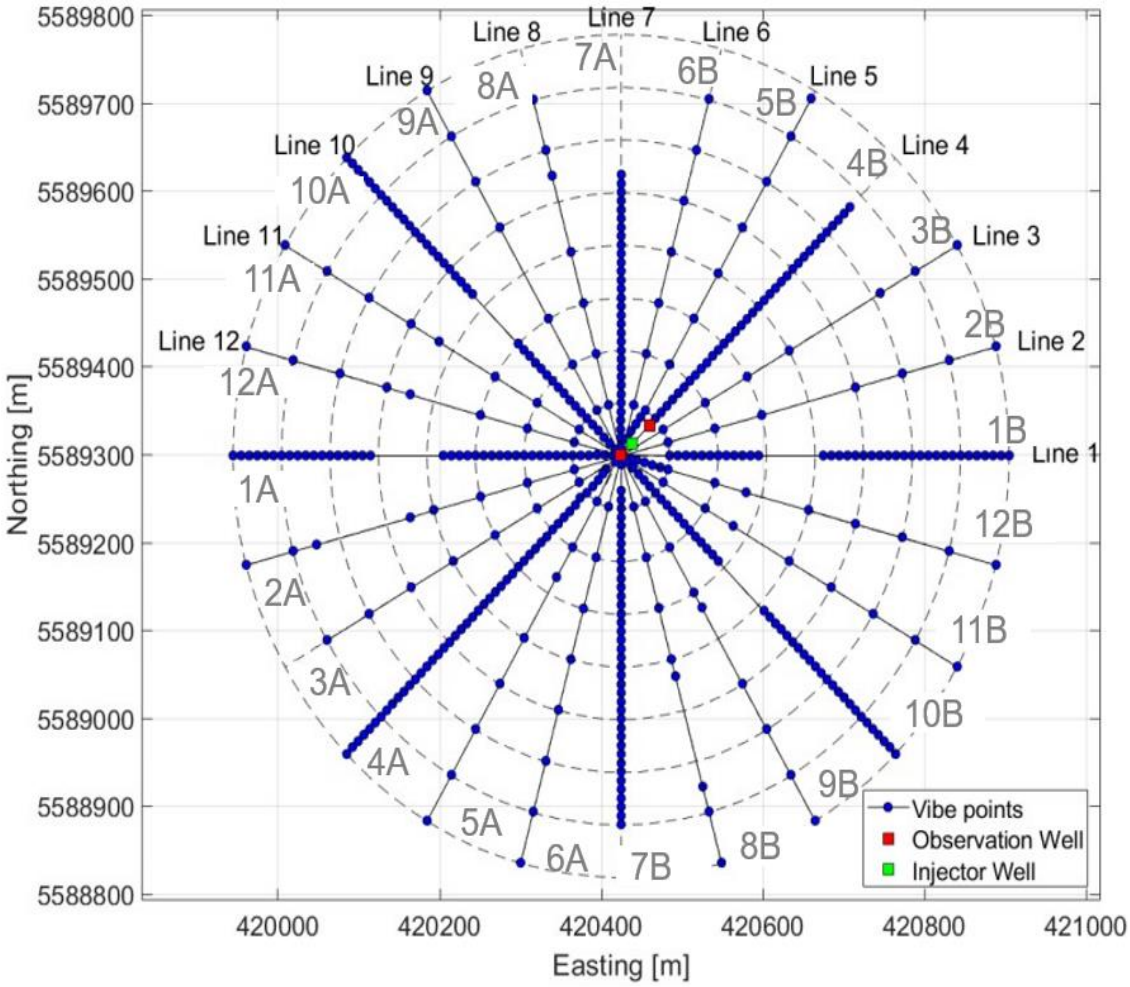

FIG. 1. Shot geometry of the CaMI-FRS 2018 3D walkaway-walkaround VSP (modified after Eaid et al., 2021).

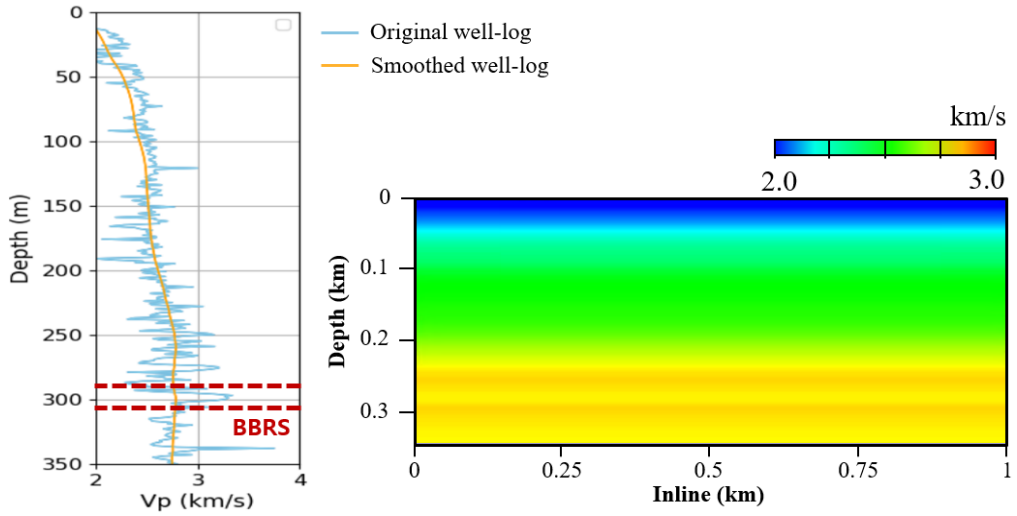

FIG. 2. The depth profile of the well-log velocity and the cross-section of the smoothed initial model along the line 7.

Figure 3 displays the vertical acceleration of the Snowflake I & II data and modelled data from the initial model. Total 9 shot gathers are regularly extracted along shot line 7. Although total recording time is 3 sec, we only use the data up to 0.3 sec in FWI to reduce computational costs. In field data, we can clearly observe the reflection events from BBRS before and after injection.

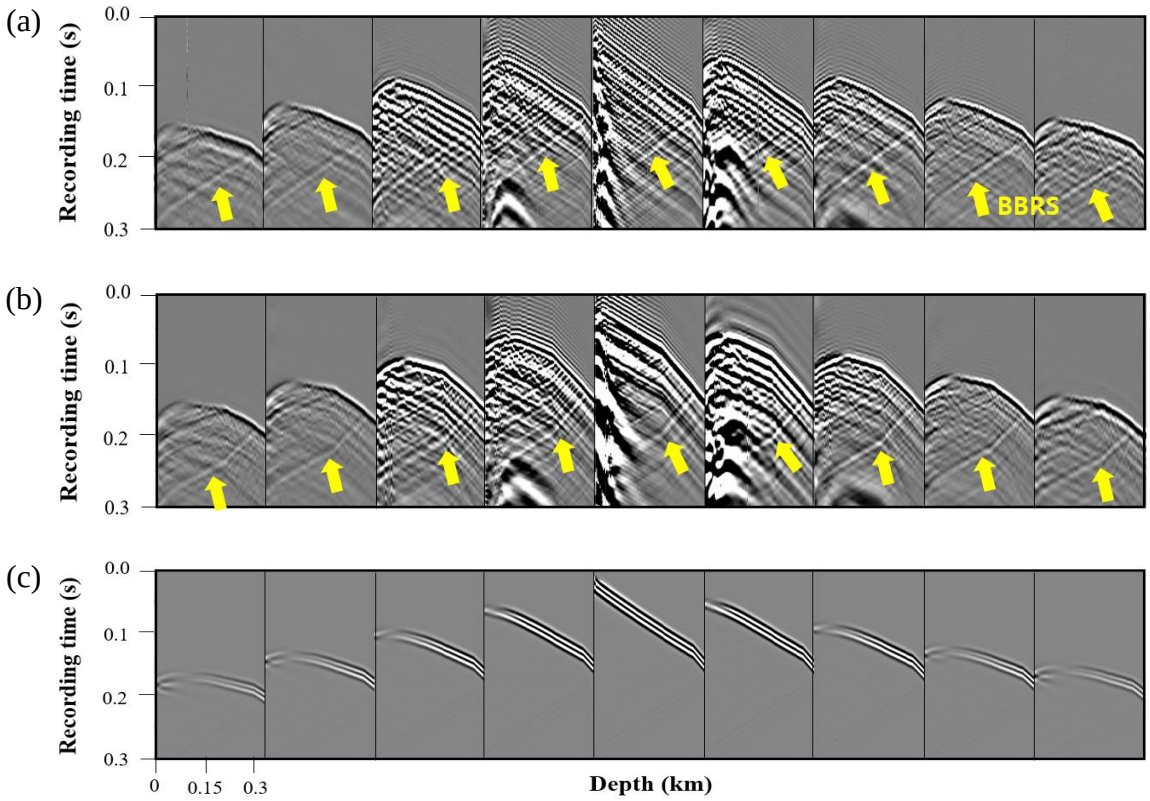

FIG. 3. The vertical components (acceleration) of (a) Snowflake I data (2018), (b) Snowflake II data (2022) and (c) modelled data. Total 9 shot gathers are regularly extracted along shot line 7.

ACOUSTIC FULL-WAVEFORM INVERSION

As we mentioned, applying elastic FWI on the 3D land seismic data requires significant computational costs. Therefore, in this work, we only consider 3D acoustic FWI to validate the applicability of 4D seismic monitoring to Snowflake data. Although there have been great improvements to enhance the applicability of 3D acoustic FWI to real seismic data, the 3D FWI for the land VSP data still suffers from several issues: (I) amplitude mismatching, (II) poor S/N ratio and (III) computational costs.

To overcome the above issues, we first choose the global correlation norm (GCN) as an objective function between modelled (u) and field (d) data in time domain, which is expressed by (Choi and Alkhalifah, 2012),

$$E(\mathbf{m}) = \sum_s \sum_r \left[-\hat{u}(s,r,\mathbf{m}) \cdot \hat{d}(s,r) \right], \tag{1}$$

where

$$\hat{u}(s,r,\mathbf{m}) = \frac{u(s,r,\mathbf{m})}{\left\|u(s,r,\mathbf{m})\right\|} \quad \text{and} \quad \hat{d}(s,r) = \frac{d(s,r)}{\left\|d(s,r)\right\|}. \tag{2}$$

The terms *s* and *r* denote the source and receiver, respectively. The parameter **m** represents the model parameter, P-wave velocity, in the subsurface media. The global correlation norm in FWI has several benefits for the land VSP data. As reported by Choi and Alkhalifah (2012), GCN is similar to phase-only inversion in the frequency domain. In addition, thanks to the normalization in equation (2), we can automatically reduce the influence of noisy traces due to the receiver malfunction. By taking the partial derivative with respect to the model parameter, we obtain the gradient direction as expressed by

$$\frac{\partial E(\mathbf{m})}{\partial m_i} = \sum_s \sum_r \left[\frac{\partial u(s,r,\mathbf{m})}{\partial m_i} \cdot b(s,r,\mathbf{m}) \right], \tag{3}$$

with the adjoint source given by

$$b(s,r,\mathbf{m}) = \frac{1}{\left\|u(s,r,\mathbf{m})\right\|} \left\{ \hat{u}(s,r,\mathbf{m})[\hat{u}(s,r,\mathbf{m}) \cdot \hat{d}(s,r)] - \hat{d}(s,r) \right\}. \tag{4}$$

The calculation of equation (3) requires huge computational costs. Therefore, we apply the adjoint-state method (Plessix, 2006) to reduce the number of forward modeling. For only 3D acoustic FWI in this work, we chose the boundary value reconstruction (Xu et al., 1995) to avoid storing huge source wavefields.

INVERSION RESULTS

The versatility of walkaway-walkaround VSP acquisition extends the applicability of Snowflake data to be applicable for both 2D and 3D FWI applications. In this section, we undertake a comparative analysis of the 2D and 3D acoustic FWI results for Snowflake I and II dataset. Initially, we present the 2D acoustic FWI results along each shot line and then we show the 3D acoustic FWI results using complete 3D VSP dataset. To ensure a fair comparison, we utilize nearly identical inversion parameters for both 2D and 3D FWI, with the exception of adopting boundary value reconstruction for 3D FWI to mitigate computational costs.

For 3D FWI, the model size is set to 1 km×1 km×0.35 km with a 5 m grid spacing. A ricker source wavelet, whose peak frequency is 100 Hz, was employed. Total number of shots are 445 (Snowflake I data) and 441 (Snowflake II data), respectively. For 2D FWI, field data are extracted along each shot line and the model size is set to 1 km×0.35 km with a 5 m grid spacing following the outermost circle in Figure 1.

In both 2D and 3D FWI, we apply a fixed steplength (0.02 km/s), after adopting the pseudo-Hessian (Shin et al., 2001) and normalizing the gradient direction. To mitigate vertical artifacts near borehole, we smooth the gradient direction only along the lateral directions, using a smoothing window of 25 m for each direction. Additionally, to enhance the far-offset reflections, we apply exponentially increasing weighting factor depends on the horizontal offsets between the source and receiver.

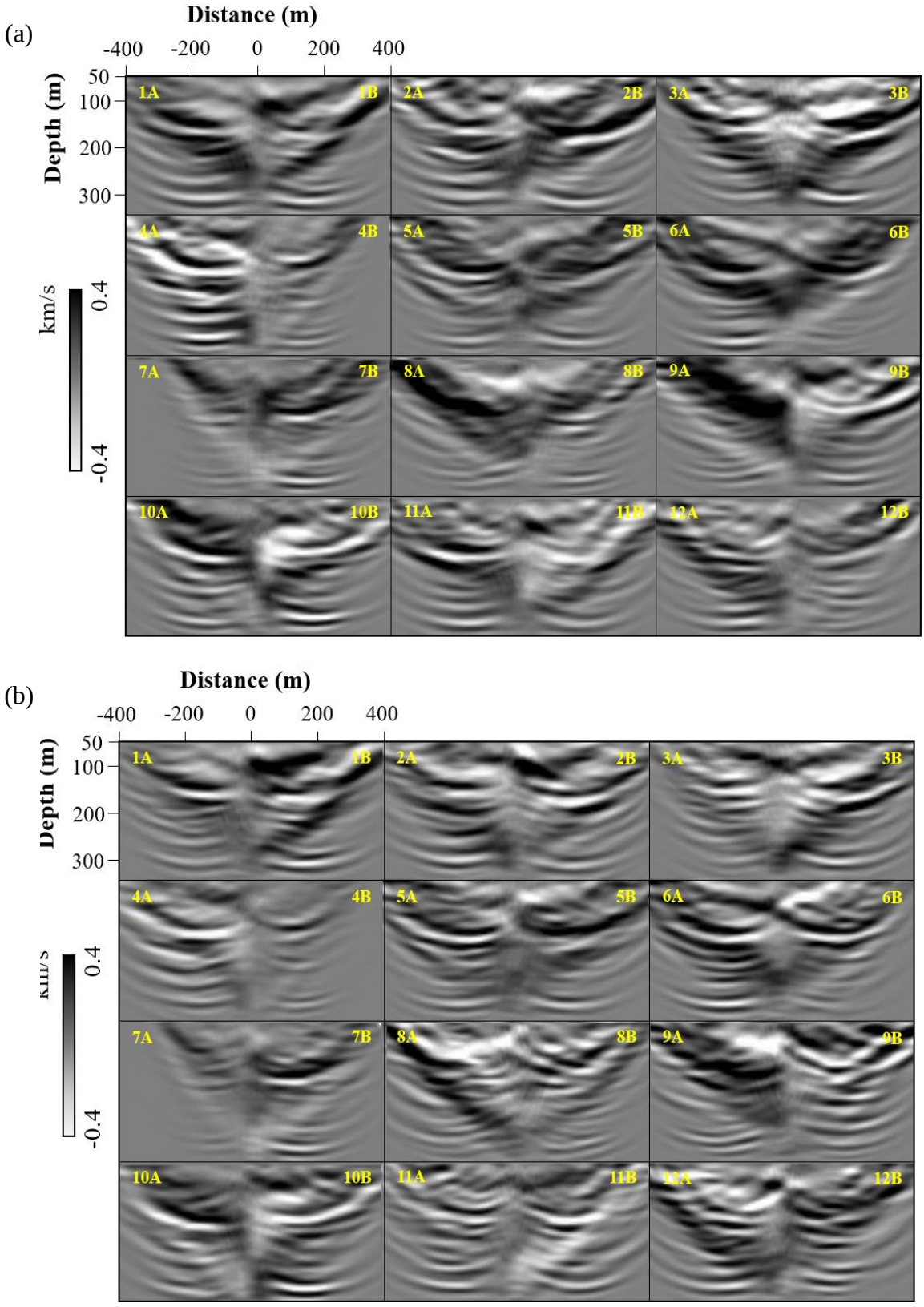

FIG. 4. The first-iteration gradient direction using 2D acoustic FWI of (a) Snowflake I data (before injection in 2018) and (b) Snowflake II data (after injection in 2022) along each survey line.

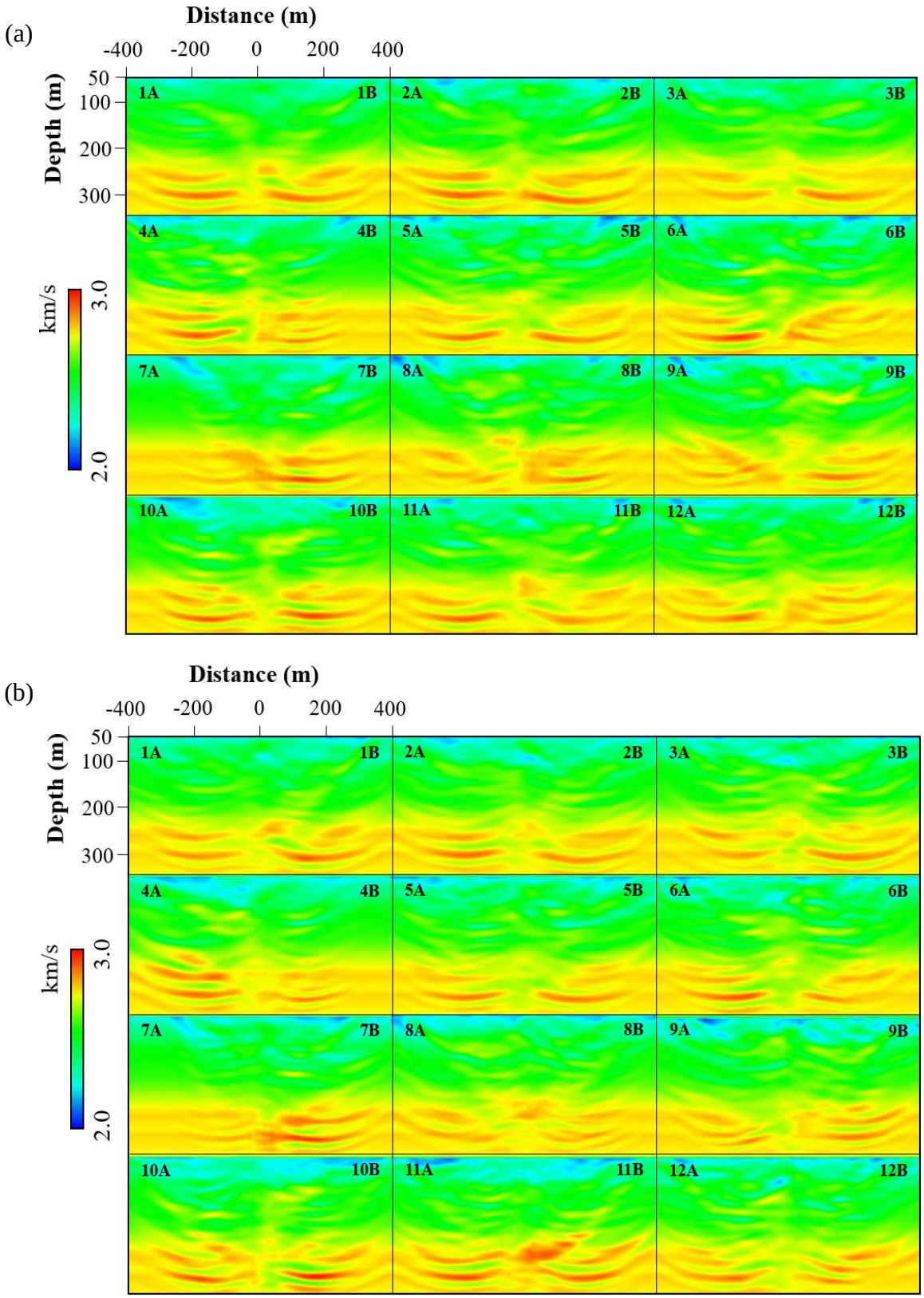

FIG. 5. The final inverted models using 2D acoustic FWI of (a) Snowflake I data (before injection in 2018) and (b) Snowflake II data (after injection in 2022) along each survey line.

We first show the gradient direction (Figure 4) and final inverted model at 15th iteration (Figure 5) from 2D acoustic FWI along each shot line of Snowflake I and II data. Along the four main lines (1, 4, 7, 10), horizontal reflectors around the borehole are clearly observable, despite the presence of nearly vertical long-wavelength updates resulting from the direct and refracted waves from the sources to borehole receivers. However, along the other lines, where fewer sources (approximately 15) are activated, the reflectors still resemble migration isochrones, leading to unsatisfactory layer continuity in the inverted models. As the FWI for Snowflake II data faces similar challenges, identifying areas with a reduction in P-wave velocity due to CO_2 injection becomes challenging. Additionally, determining the azimuthal directivity of the injected CO_2 plume is also difficult. Nevertheless, in the modelled data derived from final inverted model (Figure 6), a noticeable improvement is observed after FWI in terms of data matching.

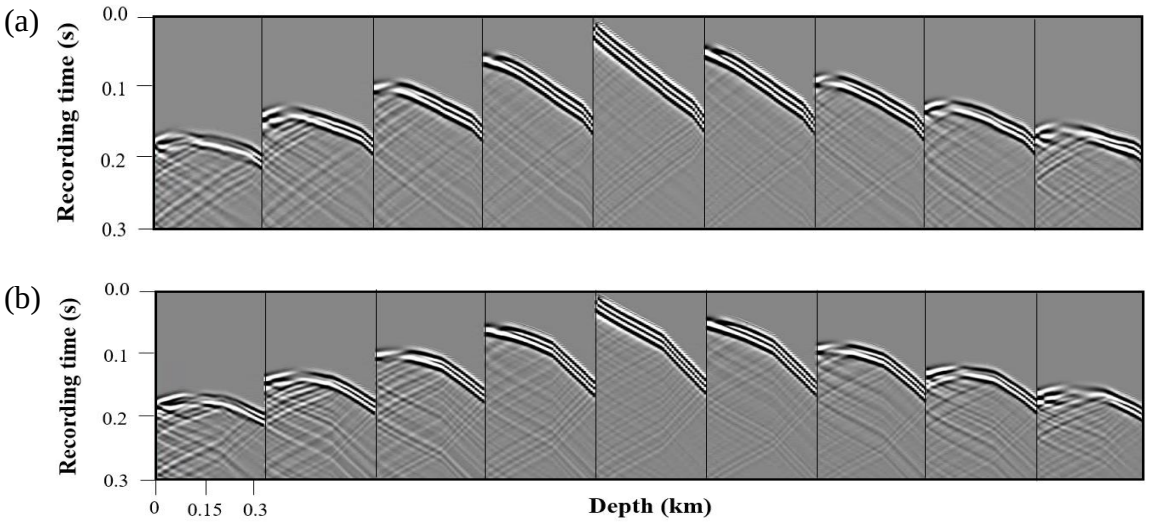

FIG. 6. The vertical components (acceleration) of modelled data from the inverted model using 2D acoustic FWI for (a) Snowflake I and (b) Snowflake II data. Total 9 shot gathers are regularly extracted along shot line 7.

We present the gradient direction (Figure 7) and final inverted model at 15th iteration (Figure 8) from 3D acoustic FWI using complete 3D VSP data. The gradient directions and inverted models from individual 3D FWI for Snowflake I and II dataset appear quite similar, enhancing the potential to detect injected CO_2 plume. Compared to the results from 2D FWI, layer continuity is significantly improved with fewer migration isochrones in 3D FWI, thanks to stacking of more reflection energy from wavefronts in the azimuthal direction. The data matching (Figure 9) is also improved after 3D FWI compared to the modelled data from initial (Figure 3) and inverted model from 2D FWI (Figure 6).

In Figures 10 and 11, by extracting cross-sections along each shot line from 3D gradient and velocity cubes, we directly compare these gradient directions and inverted models to those from 2D FWI (Figures 4 and 5). Although there still exist nearly vertical long-wavelength updates due to direct and refracted waves from the sources to borehole receivers, the layer continuities are significantly improved, particularly at injection zone (BBRS). Overall, layered structures coincide along the azimuthal direction, reflecting the geological characteristics of CaMI FRS.

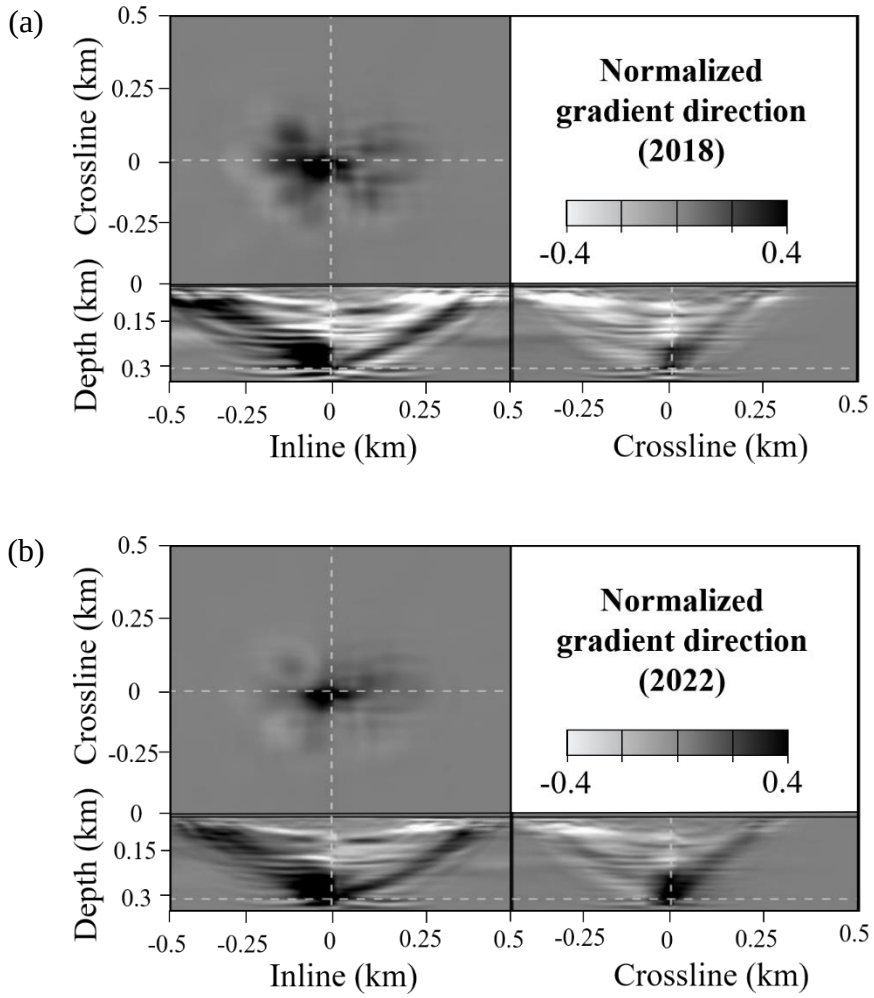

FIG. 7. The first-iteration gradient direction using 3D acoustic FWI of (a) 2018 VSP data and (b) 2022 VSP data. Two vertical slices cross the observation well.

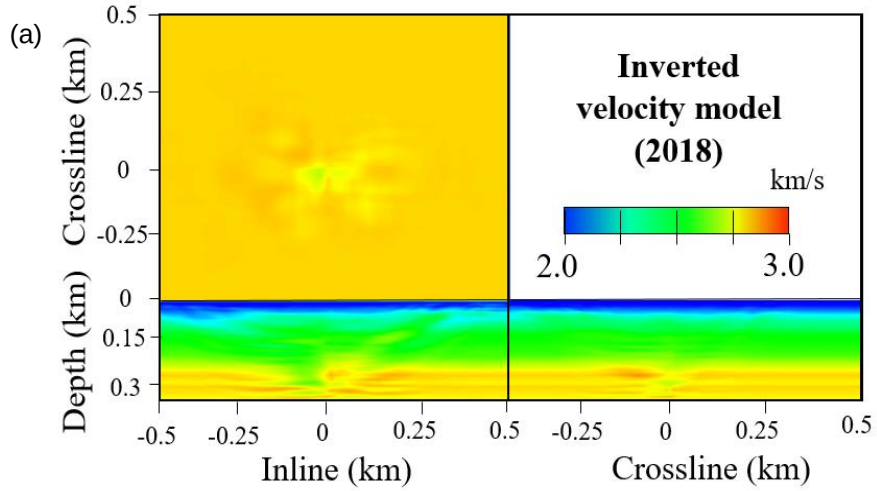

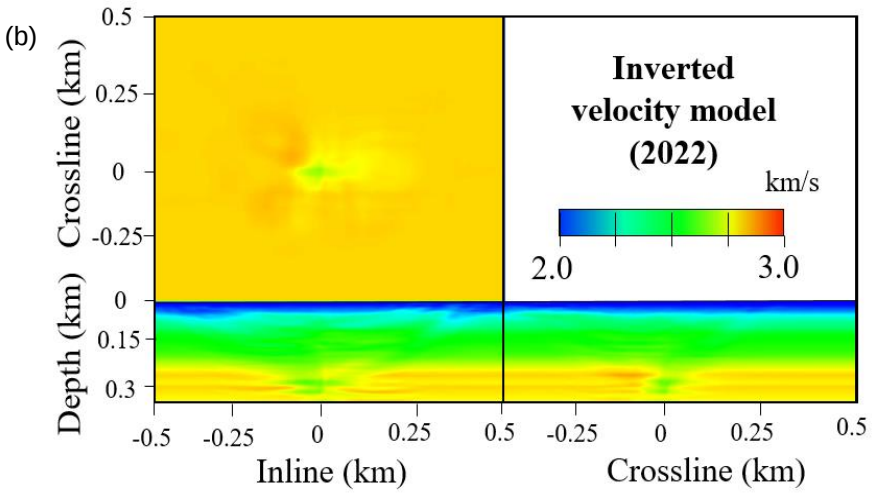

FIG. 8. The inverted velocity model using 3D acoustic FWI of (a) 2018 VSP data and (b) 2022 VSP data. Two vertical slices cross the observation well.

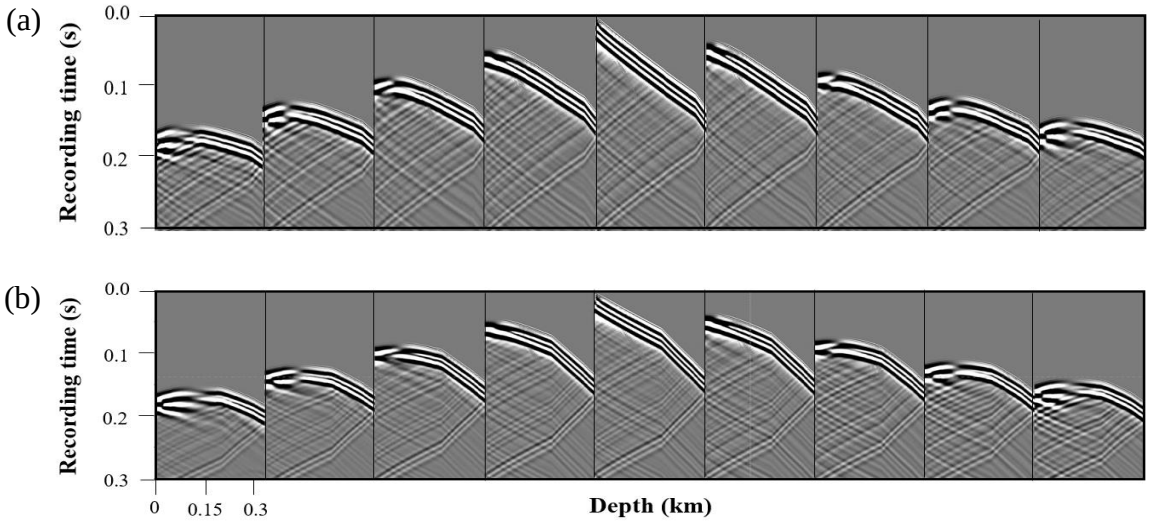

FIG. 9. The vertical components (acceleration) of modelled data from the inverted model using 3D acoustic FWI for (a) Snowflake I and (b) Snowflake II data. Total 9 shot gathers are regularly extracted along shot line 7.

We conclude by verifying the applicability of individual 3D FWI on Snowflake I and II data for monitoring injected CO_2 plume. Figure 12 displays depth slices of the velocity models at injection zone (295 m). After CO_2 injection, notable reductions in P-wave velocity are observable around both injection and observation wells. This becomes more apparent in the velocity difference, although quantitative discussion of the results is challenging due to the lateral smoothing applied to the gradient direction to mitigate vertical artifacts. Although our results offer valuable insights, further research is necessary to enhance the confidence in 4D seismic monitoring results for the Snowflake dataset. Primarily, removing or utilizing the nearly vertical long-wavelength updates will be crucial. Because raw Snowflake dataset are used in this work, preprocessing and 4D regularization may improve the results by minimizing ambient and 4D noises. Additionally, considering elastic FWI can be beneficial for quantitative monitoring.

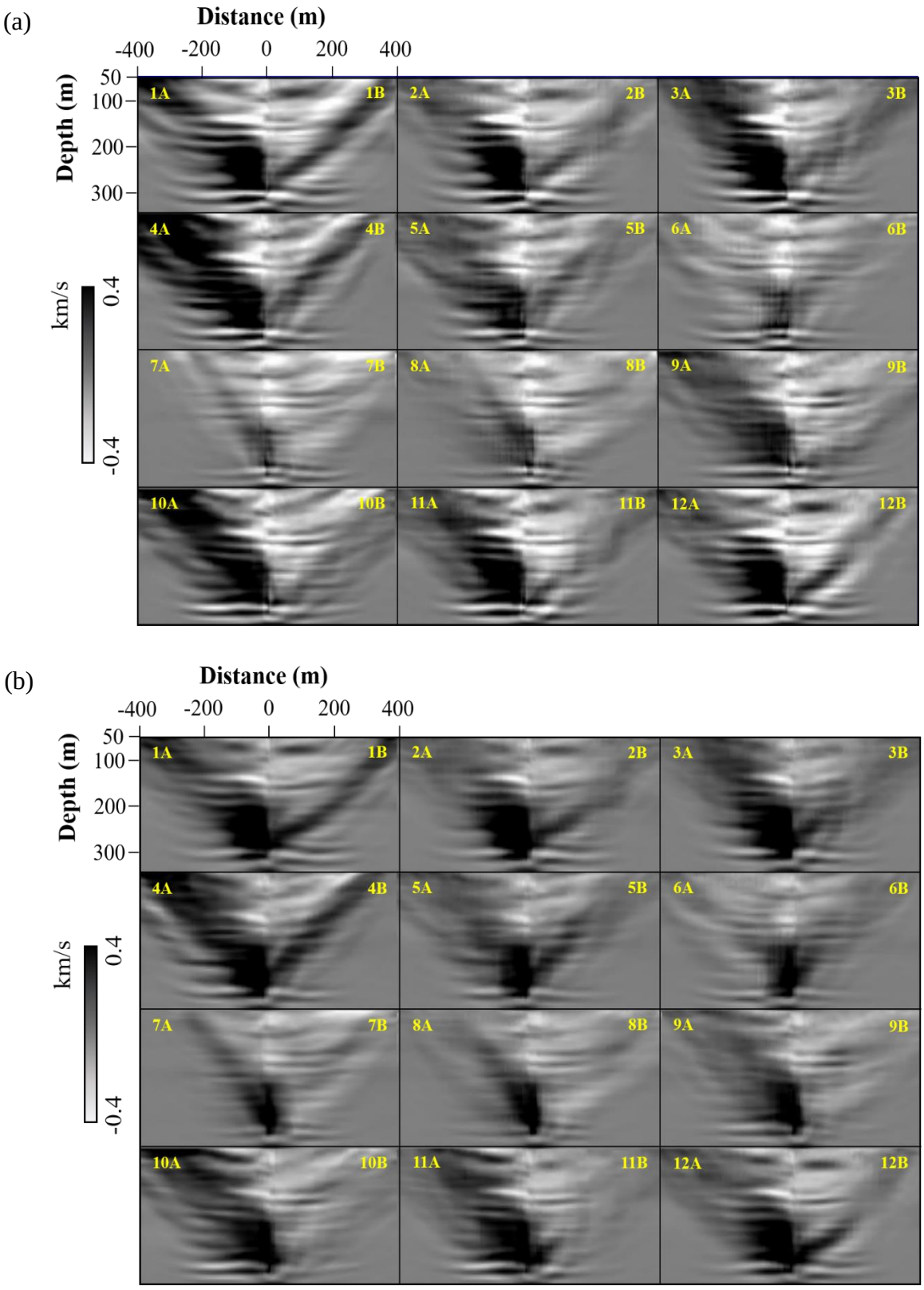

FIG. 10. The first-iteration gradient direction using 3D acoustic FWI of (a) Snowflake I data (before injection in 2018) and (b) Snowflake II data (after injection in 2022).

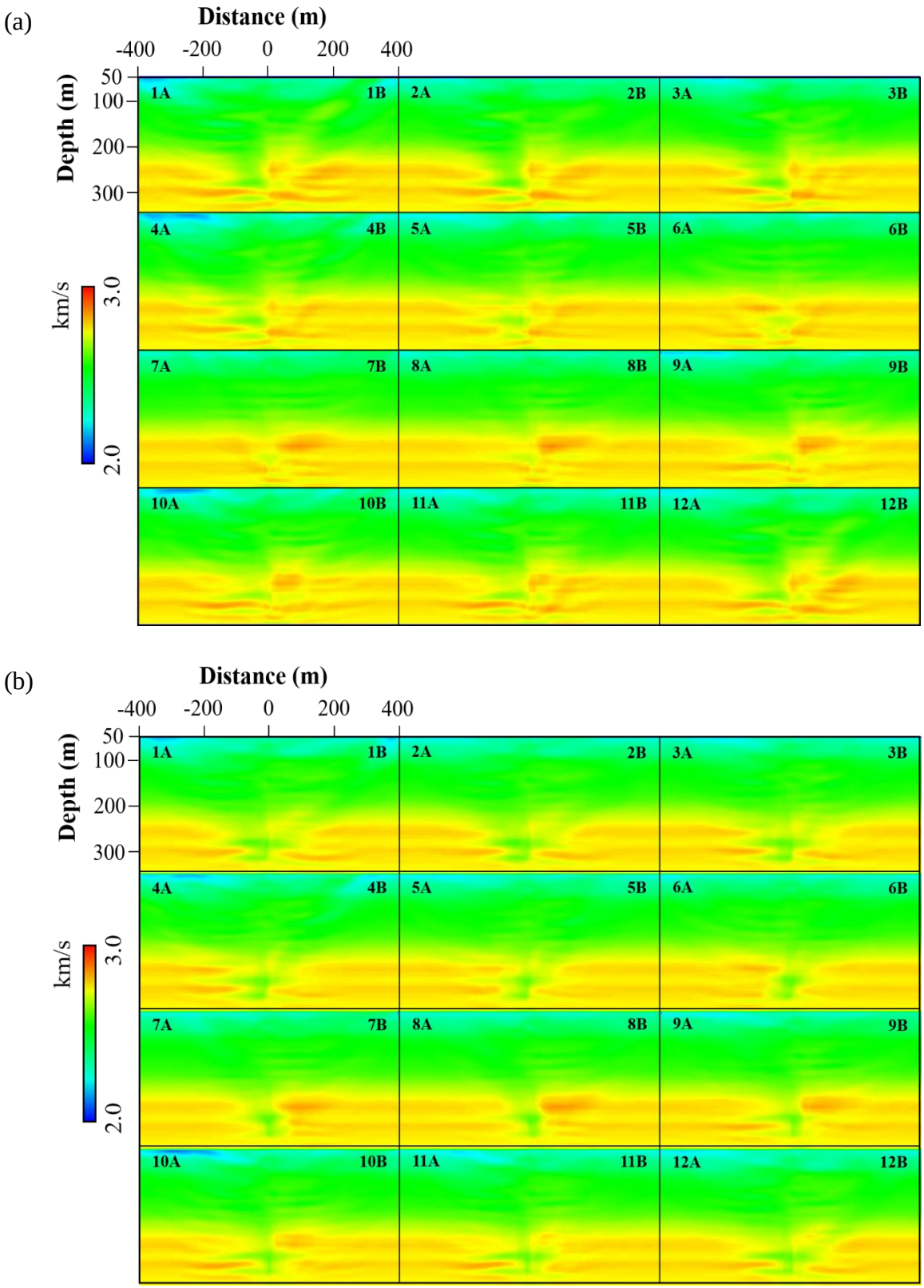

FIG. 11. The final inverted models using 3D acoustic FWI of (a) Snowflake I data (before injection in 2018) and (b) Snowflake II data (after injection in 2022).

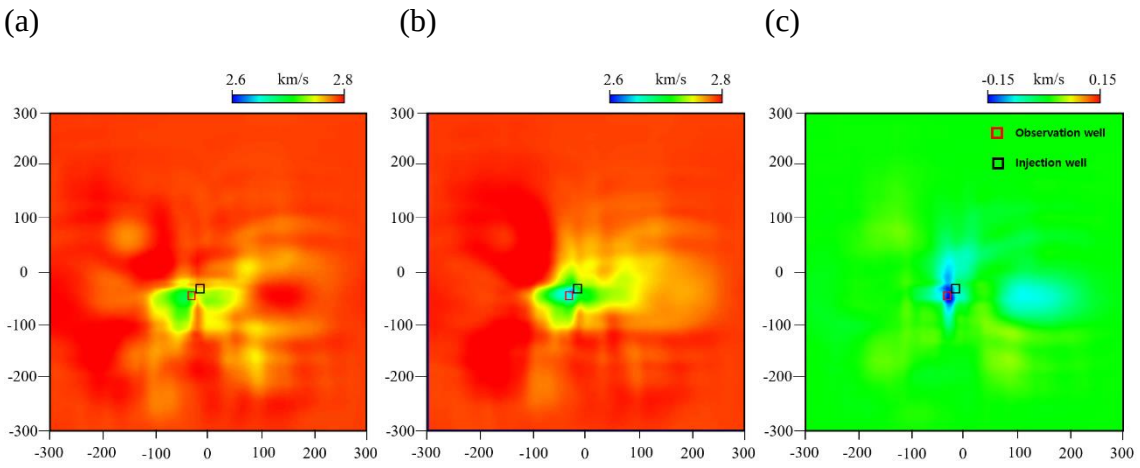

FIG. 12. The depth slices at injection zone (295 m) from inverted models for (a) Snowflake I (before injection) and (b) Snowflake II data (after injection) and (c) their difference.

CONCLUSIONS

We have validated the suitability of 3D acoustic FWI for inverting Snowflake VSP data obtained from CaMI FRS both before and after CO_2 injection. The utility of walkaway-walkaround VSP acquisition renders the Snowflake data suitable for both 2D and 3D FWI applications. Initially, we compared the results of 3D acoustic FWI with those of 2D acoustic FWI along each shot line affirming that 3D acoustic FWI provides a more satisfactory geological representation in terms of layer continuity and noise reduction.

Through individual 3D acoustic FWI for Snowflake I and II data, we verified that a reduction in P-wave velocity at injection zone is partially detected. Although the results offer valuable insights, further research is required to enhance the confidence in 4D seismic monitoring results for the Snowflake dataset. Prospective investigations should focus on refining FWI algorithms to construct improved background models, and the application of 4D regularization may enhance results by minimizing 4D noise. Additionally, considering elastic FWI for quantitative 4D monitoring could prove beneficial. However, we believe that this study serves as a foundational guide for future 4D seismic monitoring endeavors involving Snowflake data from CaMI FRS.

ACKNOWLEDGEMENTS

The sponsors of CREWES are gratefully thanked for continued support. This work was funded by CREWES industrial sponsors and NSERC (Natural Science and Engineering Research Council of Canada) through the grant CRDPJ 543578-19. This work was also supported by the Korea Institute of Energy Technology Evaluation and Planning (KETEP) and the Ministry of Trade, Industry & Energy (MOTIE) of the Republic of Korea (No. RS-2023-00249135). The data were acquired through a collaboration with the Containment and Monitoring Institute, Carbon Management Canada.

REFERENCES

Amundaray, N., Innanen, K. A., Macquet, M., and Lawton, D. C., 2020, FWI time-lapse monitoring of CO_2 injection using VSP at CaMI FRS: a feasibility study: CREWES Research Report, 32, 1.

Cai, X., Innanen, K. A., Zhang, T., Hall, K. W., and Eaid, M., 2022, Analysis of the FWI workflow for geophone and DAS data from the 2018 CaMI VSP survey: CREWES Research Report, 34, 6.

Choi, Y., and Alkhalifah, T., 2012, Application of multi-source waveform inversion to marine streamer data using the global correlation norm: Geophysical Prospecting, 2012, **60**, No. 4, 748-758.

Eaid, M., Keating, S., and Innanen, K. A., 2021, Full waveform inversion of DAS field data from the 2018 CaMI VSP survey: CREWES Research Report, 33, 7.

Egorov, A., Bóna, A., Pevzner, R., Glubokovskikh, S., and Tertyshnikov, K., 2018, Application of time-lapse full waveform inversion of vertical seismic profile data for the identification of changes introduced by CO_2 sequestration, *in* 1st Australasian Exploration Geoscience Conference – Exploration Innovation Integration, vol. 2018, 1-5.

Hall, K. W., Bertram, K. L., Bertram, M. B., Innanen, K. A., and Lawton, D. C., 2018, CREWES 2018 multi-azimuth walk-away VSP field experiment: CREWES Research Report, 30, 16.

Hu, Q., and Innanen, K. A., 2022, Bayesian approaches to estimating rock physics properties from seismic attributes: CREWES Research Report, 34, 23.

Hu, Q., Eaid, M., Keating, S., and Innanen, K. A., 2022, Quantitative FWI characterization and monitoring of reservoir properties at the CMC Newell County Facility: CREWES Research Report, 34, 22.

Macquet, M., Lawton, D. C., Saeedfar, A. A., and Osadetz, K. G., 2019, A feasibility study for detection thresholds of CO_2 at shallow depths at the CaMI Field Research Station, Newell County, Alberta, Canada: Petroleum Geoscience, **25**, No. 4., 509-518.

Plessix, R.-E., 2006, A review of the adjoint-state method for computing the gradient of a functional with geophysical applications: Geophysical Journal International, **167**, No. 2, 495-503.

Shin, C., Jang, S., and Min, D. J., 2001, Improved amplitude preservation for prestack depth migration by inverse scattering theory: Geophysical Prospecting, **49**, No. 5, 592-606.

Tarantola, A., 1984, Inversion of seismic reflection data in the acoustic approximation: Geophysics, **49**, No. 8, 1259-1266.

Xu, T., McMechan, G. A., and Sun, R., 1995, 3-D prestack full-wavefield inversion: Geophysics, **60**, No. 6, 1805-1818.